THE JOURNAL OF PHYSICAL CHEMISTRY A LETTERS

2005, *109,* 7339−7342
Published on Web 07/20/2005

Novel Cage Clusters of MoS_2 in the Gas Phase

D. M. David Jeba Singh,[†] T. Pradeep,*[,†] Joydeep Bhattacharjee,[‡] and U. V. Waghmare*[,‡]

Unit on Nanoscience and Technology (UNANST-DST), Department of Chemistry and Sophisticated Analytical Instrument Facility, Indian Institute of Technology Madras, Chennai 600 036, India, and Theoretical Sciences Unit, Jawaharlal Nehru Centre for Advanced Scientific Research, Jakkur PO, Bangalore 560 064, India

Received: May 11, 2005; In Final Form: July 5, 2005

Laser evaporation of MoS_2 nanoflakes gives negatively charged magic number clusters of compositions $Mo_{13}S_{25}$ and $Mo_{13}S_{28}$, which are shown to have closed-cage structures. The clusters are stable and do not show fragmentation in the post-source decay analysis even at the highest laser powers. Computations suggest that $Mo_{13}S_{25}$ has a central cavity with a diameter of 4.5 Å. The nanosheets of MoS_2 could curl upon laser irradiation, explaining the cluster formation.

Introduction

Inorganic molecular structures such as polyoxomolybdates are fascinating not only because of their architecture,[1] but also because of their ability to form self-organized structures.[2] In recent years, large cage structures known as inorganic fullerenes (IFs) have become an active subject of investigation.[3] IFs were originally made from layered metal chalcogenides, MX_2, where M = Mo, W and X = S, Se.[4] Later, layered metal halides such as $NiCl_2$, $CdCl_2$, and $TlCl_3$[5] and oxides such as TiO_2 and V_2O_5 were also shown to produce IFs.[6] Boron nitride also forms IFs.[7] The hollow cage structure of IFs imparts elasticity, and the materials can work as novel lubricants under various conditions.[4f] The sheetlike structure of these chalcogenides, similar to graphite, suggests that a mechanism similar to that of fullerenes and carbon nanotubes may be operative in the formation of IFs. The unsatisfied valencies present at the periphery of the layered structure makes it unstable at finite dimensions. For the layered structure of graphite to fold and form cages or closed cylinders, high energy is needed, which can be provided by laser vaporization,[8] arc discharge,[9] or other means. Ultrasound irradiation can be used for the synthesis of IFs.[10] In all methods described above, the IFs formed were in the solid state. A recent report suggested that the formation of IFs in liquid medium was achieved by laser ablation.[11] Formation of onions and nanorods of GaS by laser ablation was reported recently.[12] Zak et al.[13] reported the synthesis of MoS_2-based IFs in the gas phase, which were subsequently analyzed in the solid state. The encapsulation of WC into an IF of WS_2 was reported, showing that IFs are cagelike.[14] Structures such as octahedron, dodecahedron, and triangular prism have been proposed,[15] but a single molecular cage has not been reported so far.[16] We explored the possibility of making magic cage clusters containing Mo, W, and S in the gas phase. Initial results of this investigation are reported here.

* Corresponding authors. E-mail: (T.P.) pradeep@iitm.ac.in; (U.V.W.) waghmare@jncasr.ac.in.
[†] Indian Institute of Technology Madras.
[‡] Jawaharlal Nehru Centre for Advanced Scientific Research.

Experimental and Computational Details

Bulk MoS_2 and WS_2 were ground well to form particles of 20-μm diameter, dispersed in acetone, and spotted on the target plate of a Voyager DE PRO Biospectrometry Workstation (Applied Biosystems) matrix-assisted laser desorption ionization time-of-flight (MALDI-TOF) mass spectroscopy (MS) instrument. A pulsed nitrogen laser of 337 nm was used, and the TOF was operated in the delayed extraction mode. For fragmentation by post-source decay (PSD), as well as clustering studies, we used a timed ion selector. Isotope pattern was clearly discernible in all the cluster peaks, and a comparison of the expected and observed patterns was used to assign the peaks. The cluster peaks were significantly higher in intensity when nanosized flakes of MoS_2 were used, which were obtained by sonicating a well-ground MoS_2 sample in acetone for 10 min. A blue-colored dispersion of nanoflakes was formed, which was directly spotted on the target plate, giving a deep blue film upon drying, and laser desorption ionization (LDI) mass spectra were taken from the film. The blue material obtained by evaporation of the solvent in the dispersion was used for various spectroscopic, microscopic, and diffraction studies using standard instrumentation.

To confirm the stability of observed clusters and to understand their structures, we carried out nonempirical calculations[17] of the quantum mechanical ground state of electrons based on density functional theory with a generalized gradient approximation to the many electrons exchange correlation energy given by the Perdew−Burke−Ernzerhof (PBE) functional.[18] We used a standard plane-wave code PWSCF 2.0.1[17] with ultrasoft pseudopotentials[19] to represent the interaction between ions and electrons. An energy cutoff of 25 Ry was used on the plane-wave basis used in the representation of wave functions; the cutoff was 150 Ry for the representation of density. Structures of clusters were determined through total energy minimization using the Broyden−Fletcher−Goldfarb−Shanno (BFGS) algorithm and Hellmann−Feynman forces on atoms. In this procedure, we used different polyhedral structures as initial guesses for smaller clusters and various cage structures of sulfur atoms

10.1021/jp052454u CCC: $30.25

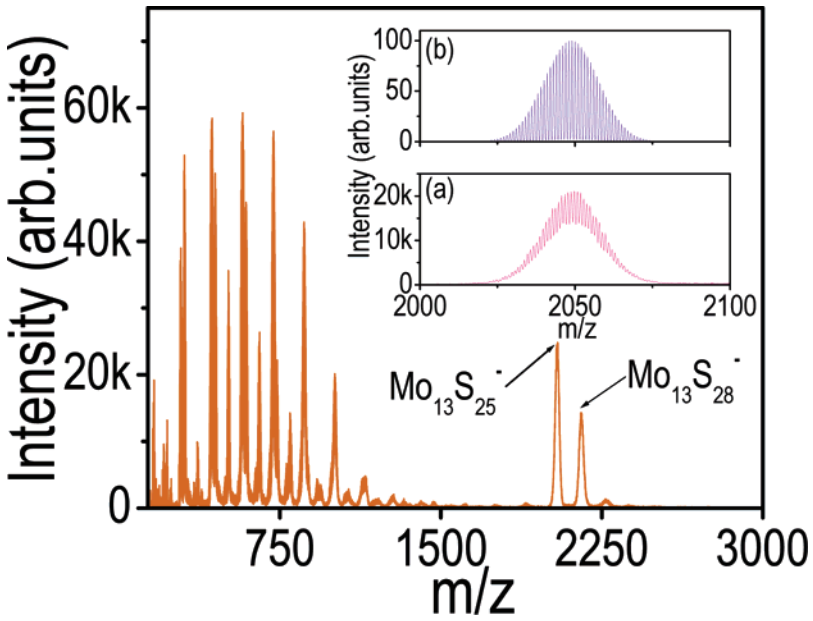

Figure 1. LDI mass spectrum of MoS_2 nanoflakes in the negative mode. Inset: Experimental spectrum taken from nanoflakes (a) shows the expected isotope distribution for $Mo_{13}S_{25}^-$ (b).

with Mo atoms located on an inner shell at positions with four- to sixfold sulfur coordination as initial guesses for larger clusters. A large supercell was used with periodic boundary conditions with a vacuum of at least 10 Å separating periodic images and a single *k*-point (0, 0, 0) as Bloch vector.

Results and Discussion

The negative-ion mass spectrum of the MoS_2 clusters obtained from the blue film is shown in Figure 1. The clusters formed are MoS_2^-, MoS_3^-, MoS_4^-, $Mo_2S_3^-$, $Mo_2S_5^-$, $Mo_2S_6^-$, $Mo_2S_8^-$, and so on. Isotope patterns matched exactly for all the clusters up to *m*/*z* ~2000. Even in very pure samples of MoS_2 and WS_2, $M_nO_y^-$ clusters were observed in poor intensity, possibly due to the presence of oxide impurities in the material. The spectra exhibit a trend: The intensity increases starting from MoS_2^-, reaches a maximum around $Mo_4S_7^-$, and decreases thereafter. Beyond this region, the spectrum is featureless till *m*/*z* 2000, and suddenly, a magic peak appears with a maximum at *m*/*z* 2049, followed by another peak at *m*/*z* 2144. The isotope pattern of the peak at *m*/*z* 2049 is shown in the inset, which matches with the expected pattern of $Mo_{13}S_{25}$. On the basis of the expected patterns and the mass numbers, we assigned the magic peaks to $Mo_{13}S_{25}^-$ and $Mo_{13}S_{28}^-$, respectively. Following these, there are some less intense peaks attributed to clusters of Mo_{14} and Mo_{15}.

When a finely ground sample dispersed in acetone is spotted on the sample plate, two regions are seen. A typical view of the sample spot as seen by a video camera is shown in Supporting Information. The center region is composed of bulk MoS_2, which is black in color. The periphery is composed of several blue spots due to the nanoflakes. We get a spectrum similar to the one shown in Figure 1 when the flakes are irradiated.

The stability of the ions was checked by PSD. The ion $Mo_{13}S_{25}^-$ did not show any fragmentation (Figure 2). Even at the highest laser power, no fragmentation was observable. However, $Mo_{13}S_{28}^-$ showed (inset of Figure 2) two fragment peaks at $Mo_{13}S_{26}^-$ (*m*/*z* 2081) and $Mo_{11}S_{19}^-$ (*m*/*z* 1664). All the smaller clusters such as $Mo_3S_7^-$, $Mo_4S_6^-$, and so on showed well-defined fragmentation patterns (data in Supporting Information). The $Mo_{13}S_{25}^-$ and $Mo_{13}S_{28}^-$ clusters were unique and were found only in the negative ion mode.

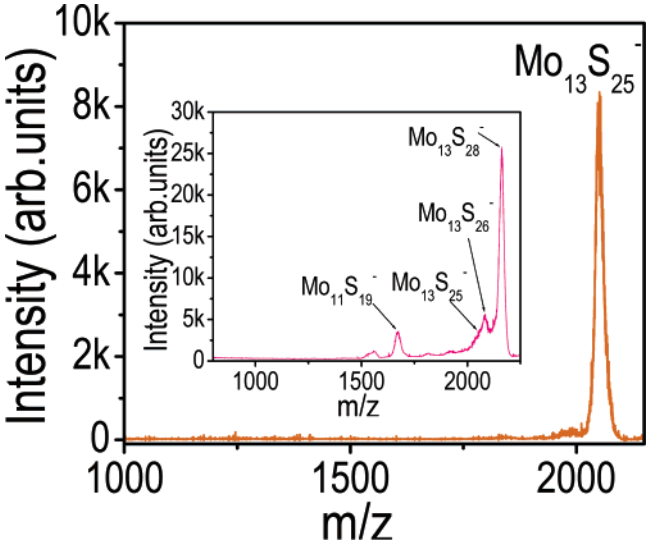

Figure 2. PSD mode LDI mass spectrum of $Mo_{13}S_{25}^-$ showing no fragmentation. Inset: PSD mode LDI mass spectrum of $Mo_{13}S_{28}^-$ showing fragmentation.

Instead of the flakes, if we irradiate bulk MoS_2, we get a spectrum as shown in Figure 3. Note that the magic peaks are barely detected. Most of the lower clusters are observed, but intensity, in general, is poor.

The blue sample collected, both by scratching the periphery of the sample spot as well as by sonicating bulk MoS_2, was analyzed using UV−visible spectroscopy (UV−vis), powder X-ray diffraction (XRD), transmission electron microscopy (TEM), energy-dispersive X-ray analysis (EDAX), Fourier transform infrared spectroscopy (FT-IR), and Raman spectroscopy under identical conditions. These investigations were done to characterize the nature of the starting material, as other forms of molybdenum blues are known in the literature.[1] The X-ray diffractogram shows the (002) reflection of MoS_2, and Mo and S features in the expected atomic ratio are shown in EDAX (Figure 4a). The material therefore is MoS_2 itself, in the nanodimension with a particle size of ~60−70 nm (Figure 4b).

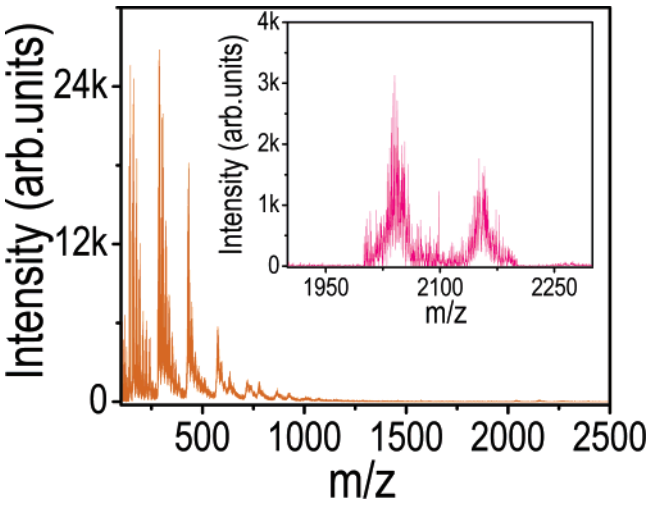

Figure 3. LDI mass spectrum of bulk MoS_2. Inset: Zoomed (25×) portion of the same spectrum showing $Mo_{13}S_{25}^-$ and $Mo_{13}S_{28}^-$ with very low intensity.

Characteristic E^1_{2g} and A_{1g} modes of MoS_2 appear in the Raman spectrum at 381 and 406 cm^{-1}, respectively (ref 20). It appears that thinner flakes with fewer layers are easier to get evaporated, which could be curling to form the cagelike structures. All the other data are presented in the Supporting Information.

The possibility of formation of the Mo_{13} clusters by aggregation of smaller clusters was investigated using the timed ion selector. None of the smaller clusters showed features due to Mo_{13} (data in Supporting Information). This clearly indicates that the magic clusters around Mo_{13} are formed by direct laser desorption of MoS_2 layers and not due to aggregation of smaller clusters.

Calculated cohesive energies per atom (Figure 5), while expected to be overestimated, clearly show that Mo_2S_3 and $Mo_{13}S_{25}$ clusters are relatively more stable than others. Also, we note that the $Mo_{13}S_{25}$ cluster is most stable among the ones studied here. Energies needed to fragment $Mo_{13}S_{28}$ and $Mo_{13}S_{25}$ into the most stable smaller ones such as Mo_2S_3 and Mo_2S_5 are estimated to be 0.45 and 0.57 eV/atom, respectively, according to their stability. In addition, this result demonstrates greater stability for $Mo_{13}S_{25}$ than $Mo_{13}S_{28}$, consistent with the experimental observations. As no stable unusual clusters were found in the intermediate region, we did not explore them through computations.

The calculated structure of these clusters exhibits a core of Mo atoms, each with 4−6 neighboring S atoms located in an outer shell, each with 1−3 neighboring Mo atoms. The core of Mo atoms forms a cage with 12 atoms, and the 13th Mo atom is at one end forming a small tetrahedral cap. In the structure, 12 of the Mo atoms have 5 S-neighbors each, while the remaining 1 has 3 S-neighbors. Of the sulfurs, 19 have 3 Mo-neighbors each, 3 have 2 Mo-neighbors each, and the rest (3) have 1 Mo- and 1 S-neighbor each. Average sulfur coordination of Mo in $Mo_{13}S_{25}$ ($Mo_{13}S_{28}$) is 4.84 (5.0). The structure of $Mo_{13}S_{25}$ is like a cage with an almost spherical void space with a diameter of about 4.5 Å (Supporting Information). The $Mo_{13}S_{25}$ structure has a threefold symmetry (evident in Figure 5), and its core of Mo atoms resembles a curled triangular net of Mo atoms, while that of $Mo_{13}S_{28}$ has the shape of a short cylinder, revealing significant structural relaxation and deviation from the initial spherical cagelike structure. This indicates that these clusters may have formed by curling of the MoS_2 sheets.

Examination of charge density contours (Supporting Information) reveals mixed ionic and directional bonding between Mo and S atoms. Stability of these clusters arises from mixed ionic−covalent bonding between Mo and S and electrostatic interionic interactions. Comparison of energies of MoS, MoS_2, MoS_3, and MoS_4 clusters shows that the energy of a Mo−S bond is the strongest in MoS_2, while the binding energy per atom is highest for MoS_3. Fragmentation energies of Mo_2S_3 and Mo_2S_5 clusters into MoS and MoS_3 clusters are 2.35 and 1.14 eV/atom, respectively ($2Mo_2S_3 = 3MoS + MoS_3$ and $2Mo_2S_5 = MoS + 3MoS_3$), whereas that for fragmenting Mo_2S_5 and Mo_2S_6 into MoS_2 and MoS_4 ($2Mo_2S_5 = 3MoS_2 + MoS_4$ and $Mo_2S_6 = MoS_2 + MoS_4$) are 0.74 and 0.57 eV/atom, respectively. The former are much larger than the latter because MoS itself is not very stable.

In WS_2, magic peaks were found at $W_{12}S_{20}O^-$ ($m/z = 2862$) and $W_{13}S_{22}^-$ ($m/z = 3094$). There is also an intense ion at $W_6S_9O^-$ (m/z 1407). These peaks show high stability in PSD (data in Supporting Information). Oxygenation could not be avoided despite repeated baking of the samples in Ar.

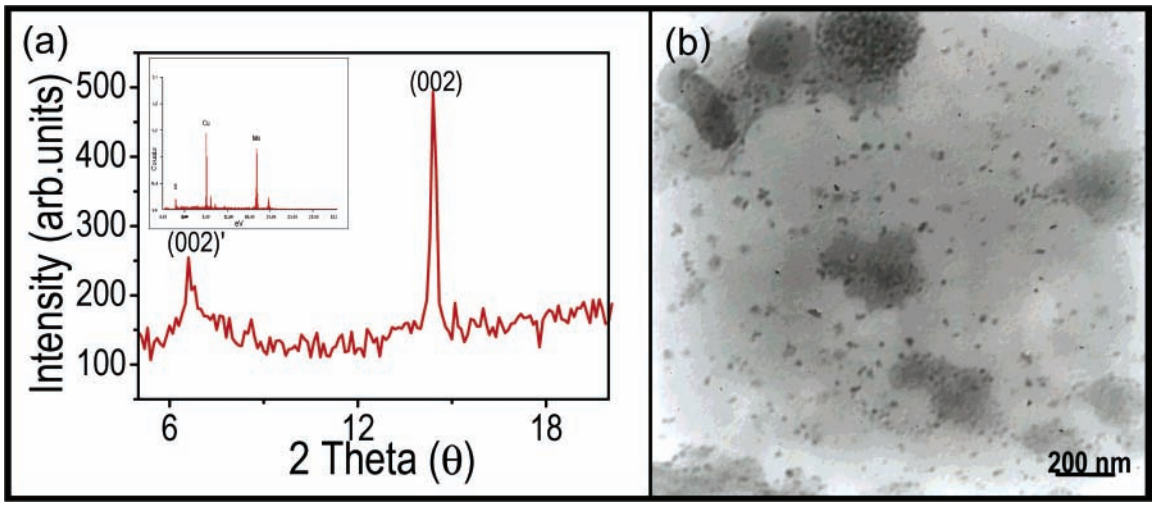

Figure 4. (a) XRD pattern of the acetone extract showing MoS_2 features. The pattern shows the presence of MoS_2 (002) plane (JCPDS no. 87-2416). Inset: EDAX analysis gave Mo and S in the expected ratio. The Cu signal is due to the copper grid used for TEM. (b) TEM of the extract. The material is composed of nanosize flakes of MoS_2. The particle size is estimated to be ~60−70 nm. The analysis was done with a 120 keV Philips CM12 instrument.

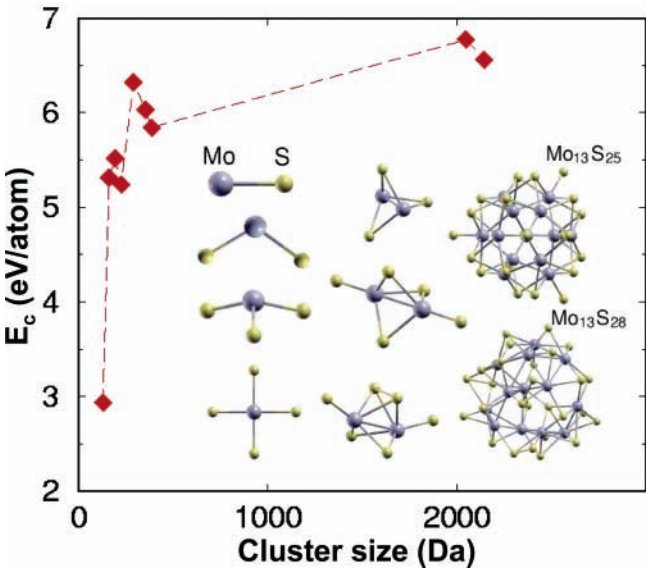

Figure 5. Calculated cohesive energies of Mo_mS_n clusters as a function of their masses. The optimized structures of these clusters are also shown.

In summary, we have shown the existence of stable negatively charged clusters of composition $Mo_{13}S_{25}$ and $Mo_{13}S_{28}$ in the gas phase. Computations confirm their structural and electronic stability. These clusters are likely to be inorganic fullerenes and may be formed by the curling of nanoflakes of MoS_2. Considering their stability, they may be formed in the condensed phase under appropriate conditions. Experimental ion mobility experiments may be useful to confirm the proposed structures.

Acknowledgment. Our nanomaterials program is supported by the Department of Science and Technology. D.M.D.J. Singh was supported by a Swarnajayanti Fellowship awarded to T.P. U.V.W. acknowledges support from a DuPont Young Faculty Award.

Supporting Information Available: Schematic view of the sample spot, PSD data of small MoS_2 clusters, their ion selection mass spectra, spectroscopic analysis of MoS_2 nanoflakes, computational results and WS_2 data. This material is available free of charge via the Internet at http://pubs.acs.org.

References and Notes

(1) Müller, A.; Serain, C. *Acc. Chem. Res*. **2000**, *33*, 2.
(2) Liu, T.; Diemann, E.; Li, H.; Dress, A. W. M.; Müller, A. *Nature (London)* **2003**, *426*, 59.
(3) Tenne, R.; Rao, C. N. R. *Philos. Trans. R. Soc. London, Ser. A* **2004**, *362*, 2099.
(4) (a) Tenne, R.; Margulis, L.; Genut, M.; Hodes, G. *Nature (London)* **1992**, *360*, 440. (b) Margulis, L.; Salitra, G.; Tenne, R.; Talianker, M. *Nature (London)* **1993**, *365*, 113. (c) Tenne, R.; Margulis, I.; Hodes, G. *Adv. Mater*. **1993**, *5*, 386. (d) Feldman, Y.; Wasserman, E.; Srolovitz, D. J.; Tenne, R. *Science* **1995**, *267*, 222. (e) Homyonfer, M.; Mastai, Y.; Hershfinkel, M.; Volterra, V.; Hutchison, J. L.; Tenne, R. *J. Am. Chem. Soc*. **1996**, *118*, 7804. (f) Rapoport, L.; Bilik, Y.; Feldman, Y.; Homyonfer, M.; Cohen, S. R.; Tenne, R. *Nature (London)* **1997**, *387*, 791. (g) Homyonfer, M.; Alperson, B.; Rosenberg, Y.; Sapir, L.; Cohen, S. R.; Hodes, G.; Tenne, R. *J. Am. Chem. Soc*. **1997**, *119*, 2693.
(5) (a) Hacohen, Y. R.; Grunbaum, E.; Tenne, R.; Sloan, J.; Hutchison, J. L. *Nature (London)* **1998**, *395*, 336. (b) Popovitz-Biro, R.; Twersky, A.; Rosenfeld Hacohen, Y.; Tenne, R. *Isr. J. Chem.* **2001**, *41*, 7.
(6) Hoyer, P. *Adv. Mater*. **1996**, *8*, 857. (b) Muhr, H. J.; Krumeich, F.; Schonholzer, U. P.; Bieri, F.; Niederberger, M.; Gauckler, L. J.; Nesper, R. *Adv. Mater*. **2000**, *12*, 231.
(7) Wang, X.; Xie, Y.; Guo, Q. *Chem. Commun*. **2003**, 2688.
(8) Kroto, H. W.; Heath, J. R.; O'Brien, S. C.; Curl, R. F.; Smalley, R. E. *Nature (London)* **1985**, *318*, 162.
(9) Kratschmer, L. D.; Lamb, K.; Fostiropoulos; Huffman, D. R. *Nature (London)* **1990**, *347*, 354.
(10) Avivi, S.; Mastai, Y.; Gedanken, A. *J. Am. Chem. Soc*. **2000**, *122*, 4331.
(11) Nath, M.; Rao, C. N. R.; Ronit, P. B.; Angi, A. Y.; Tenne, R. *Chem. Mater*. **2004**, *16*, 2238.
(12) Gautam, U. K.; Vivekchand, S. R. C.; Govindaraj, A.; Kulkarni, G. U.; Selvi, N. R.; Rao, C. N. R. *J. Am. Chem. Soc*. **2005**, *127*, 3658.
(13) Zak, A.; Feldman, Y.; Alperovich, V.; Rosentsveig, R.; Tenne, R. J. *Am. Chem. Soc*. **2000**, *122*, 11108
(14) Rothschild, A.; Sloan, J.; York, A. P. E.; Green, M. L. H.; Hutchison, J. L.; Tenne, R. *Chem. Commun*. **1999**, 363.
(15) Ascencio, J. A.; Perez-Alvarez, M.; Molina, L. M.; Santiago, P.; Jose-Yacaman, M. *Surf. Sci*. **2003**, *526*, 243.
(16) Philip, A. P.; Anne, C. D.; Bruce, A. P.; Kim, M. J.; Alleman, J.; Riker, G.; David, S. G.; Michael, J. H. *J. Phys. Chem. B* **2004**, *108*, 6197.
(17) Baroni, S.; Corso, A. D.; Gironcoli, S.; Giannozzi, P. http://www.pwscf.org.
(18) Perdew, J. P.; Burke, K.; Ernzerhof, M. *Phys. Rev. Lett*. **1998**, *80*, 891.
(19) Vanderbilt, D. *Phys. Rev. B* **1990**, *41*, 7892.
(20) Frey, G. L.; Tenne, R.; Matthews, M. J.; Dresselhaus, M. S.; Dresselhaus, G. *Phys. Rev. B* **1999**, *60*, 2883.